

A Human-Expertise Based Statistical Method for Analysis of Log Data from a Commuter Ferry

Baiheng Wu, Guoyuan Li, Luman Zhao, Hans Petter Hildre, and Houxiang Zhang

Department of Ocean Operations and Civil Engineering

Norwegian University of Science and Technology (NTNU)

Ålesund, Norway

{baiheng.wu, guoyuan.li, luman.zhao, hans.p.hildre, hozh}@ntnu.no

Abstract—The proposed method in this paper aims to better understand the log data from the commuter ferry. By the method, the mechanism of how the human expertise operates the ferry can be found, and thus help to establish ship intelligence for the autonomous commuting sailing. The log data of sailings with the same departure and arrival ports is of interest in this respect. The method defines different phases of a sailing as different scenarios in terms of the features contained in the collected data. The features are reflected by the ship behavior/response and the ship machinery/actuators. Compared to the typical sailing phases which are distinct to each other, the features can be uncertain when the ferry transfers from the current phase to the sequential. The concept of the transition time window is thus raised to interpret the uncertainty between adjacent phases. Based on the collected data, the human expertise is involved to summarize features and generate empirical criteria for the decomposition. After the whole sailing being split into a sequential-scenario series, statistical heat maps are drawn to illustrate the likelihood site with respect to the collected log data. In practice, log data collected from a customized commuting route in Trondheim are analyzed by the proposed method.

Index Terms—Data analysis, commuter ferry, autonomous surface vehicles, decision support

I. INTRODUCTION

Nowadays, although autonomous techniques are becoming increasingly popular in various industries as well as people's everyday life, it is still under development in the shipping industry, where manual work is highly demanded. Yet, it is reported that 70-90 % marine accidents are caused by human's improper operations [1][2]. Apart from potential navigation risks, the huge expenditure spent on employing on-board staff members also triggers stakeholders to invest shipping autonomy. As a result, researches on autonomous ships have gained great popularity in both industry and academia in the recent years. With the rapid development of artificial intelligence, such as data mining, machine learning, sensor fusion, and also with the hardware apparatus becoming more robust and precise, the advent of autonomous ships seems promising in the near future [3].

One of the major concerns that may hamper the appearance of autonomous ships is its uncertainty when facing unexpected situations. It is argued that, with the current ship intelligence,

autonomous ships are likely to perform well under normal circumstances [4][5]. However, their capacity to handle cases of complicated conditions, especially in the case of danger and emergency, is highly contentious. In this respect, human expertise is believed to outperform ship intelligence as humans are able to address unexpected situations synthetically based on their knowledge and experience [6][7]. Although a large proportion of marine accidents are initiated by humans, it cannot be neglected that human expertise has operated their vessels safely and successfully for innumerable sailings. Hence, unless ship intelligence is fully tested to be able to take rational action under any circumstances on-board, human operation will continue to be the best option of sailing. From this point, the mechanism of how human expertise operates vessels can set a paradigm for ship intelligence [8].

Under this background, it is suggested that ship intelligence should be applied in some simple cases first [9]. A commuter ferry that executes a regular route between two unaltered ports can be seen as a pragmatic example. A commuting route simplifies the autonomous navigation process to a large extent, for example one commuting route is usually followed by the same vessel or similar ones, and the hydrological conditions at the same location usually do not vary much, and thus can be used to test ship intelligence. A commuting route usually follows an assigned seaway at a short sailing mileage, which implies that the whole sailing procedure contains countable pivotal operations. In addition, a commuting route is usually close to the shore and the coast patrol and/or the on-call security guard in the vicinity can take immediate rescue action if an accident were to happen, which consequently reduces the risk of inducing considerable loss [10]. In a word, the commuter ferry provides one of the most ideal and applicable scenario in which ship intelligence can be facilitated.

In recent years, the value of data is getting more emphasized, as well as in the maritime field. There have been researchers utilizing the automatic identification system (AIS) data for autonomous navigation [11][12], using the on-board data to monitor the status of the ship health [13][14], or trying to find the human expertise's navigation mechanism from their behavior [15]. While, this paper emphasises the importance of log data. There are innumerable commuter ferries running in the world every minute; while compared with the pelagic ocean route, the commuting route usually

The project is financially supported by grants from the Research Council of Norway with the MAROFF KPN "Digital Twins for Vessel Life Cycle Service" (Project NO. 280703).

follows a seasonal schedule and runs more frequently. Yet, the massive quantity of data are not wisely utilized. It is previously noted that human expertise operations on-board can serve as the paradigm for ship intelligence. The scenario of the commuting route provides relatively a large amount of practice. In addition, log data often contain the key information (such as human commands, the ship motion and response, and the environmental conditions) that can be utilized to build a model that can demonstrate the whole sailing procedure explicitly [16]. Furthermore, the model can reflect the mechanism of how humans operate their vessels systematically. In return, the established mechanism can help support on-board decisions and to develop ship intelligence.

This paper suggests a method to interpret the log data from a commuter ferry. Firstly, the log data recording sailings on the commuting route are cut out from the timeline into fragments, and each fragment contains the information of one entire sailing. With this method, the sailing data are sorted into different groups (e.g. actuators and response) with respect to what the data presents. Next, the relationships between different data groups are explored and qualitatively established with respect to the advice from the human expertise. Both the features of different data groups and their relationships are used to help to divide the whole route into several scenarios. At last, a statistical heat map is drawn based on the scenario decomposed result and the locations at which critical operational commands take place.

The layout of the paper is as following: Sec. II presents the proposed method in detail, including the data collecting and pre-processing, the scenario decomposition and the definition of the transition time window, and how the data will be utilized to demonstrate the commuter sailing. Sec. III gives the results of decomposition of the log data, and also how it is interpreted by statistical analysis. A discussion about the result and the application prospect is given in Sec. IV. At last, a conclusion follows in Sec. V.

II. METHODOLOGY

The main objective of this paper is to understand how the captain maneuvers the commuter ferry during the whole sailing procedure based on the recorded log data which may reveal the interaction between the command of the captain and the situation/behavior of the ship. The analytical method with respect to the advice from the human expertise is used to extract features from the data in order to demonstrate the behavior of the ship and label its status. Statistics based on the features and the labeled status are expected to form the site of the likelihood for each of the decomposed scenarios. The flowchart of the method framework is given in Fig. 1.

A. Data collection and pre-processing

The data used in this paper are collected from a commuting route located in Trondheim, Norway. The commuting route connects the Trondhjem Biological Station and the berthing point at the estuary of the Nidelva river. The commuting route is executed by NTNU's research vessel R/V Gunnerus. The

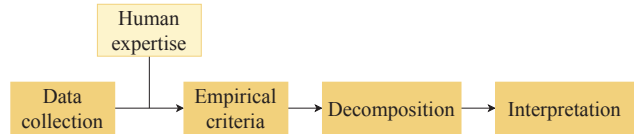


Fig. 1. Flowchart of the proposed method.

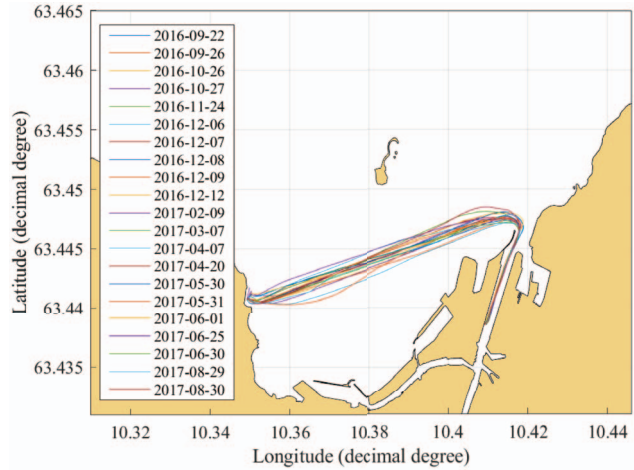


Fig. 2. Collection of 21 commuter sailings.

TABLE I
CLASSIFICATION OF LOG DATA

Ship behaviors	Machinery actuators	Environment
course (°)	engine status (0/1)	wind speed (knots)
heading (°)	bow thruster feedback (%)	wind direction (°)
speed (knots)	portboard-rpm feedback (%)	
position (°)	starboard-rpm feedback (%)	
roll (°)	portboard-Azi feedback (°)	
pitch (°)	starboard-Azi feedback (°)	

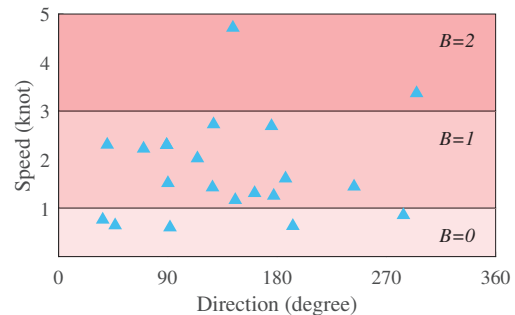


Fig. 3. Wind speed and direction in statistics.

vessel is equipped with a bow thruster for the positioning operation at 200 kW and two main azimuth thrusters, each with the propulsion at 500 kW [17]. The log data record the information of 21 sailings from September 2016 to August 2017 as shown in Fig. 2. The log data are recorded under the Unix Epoch time and then converted to the UTC system so as to make them readable. The log data are updated every second, i.e., a sampling frequency of 1 Hz.

The information contained in log data can be classified into three groups which is shown in Table I. It includes ship behaviors, machinery actuators and environment conditions. The items in the ship behaviors group follow the convention. The geographic north is denoted as 0° and increases clockwise. The location of the ferry is referred by the geographic coordinate system with the longitude and latitude. The engine status is denoted by 0 for off or 1 for on.

Two items that demonstrate the wind speed and direction are also included in collected data. By calculating the average wind speed and direction when the ship stops in the quay, the wind conditions of the 21 sailings are estimated and presented in Fig. 3. The wind speed and direction of two data sets are the same and overlap in the figure, hence there only 20 data points. It shows that the highest average wind speed is under 5 knots, which is rated at level 2 according to the Beaufort wind force scale (B in Fig. 3). As the wind at this level is often considered to have trivial effects on sailings, the wind data will not be further analyzed in this paper.

B. Decomposed scenarios' definition

After scrutinizing the data of 21 sailings, the commuting route can be intuitively decomposed into four main stages, including departing, cruising, turning and docking. There are two distinguishable phases in the docking stage, named as converging (to the shore) and bow thrusting phase respectively. The scenario sequence of the decomposition is shown as Fig. 4.

The definition of each scenario is given as follow:

- **Departing:** the ferry sets off from the port. At the beginning of this stage, the bow thruster usually starts first with the azimuth thrusters at an assigned angle and low RPM to translational push the ferry to a safe distance from the dock wall. Then the ferry will turn to the desired direction by adjusting the azimuth angle. During the turning phase, the RPM will increase to accelerate the ferry and will be loaded at the maximum value a little earlier than the ferry getting the heading for cruising direction.
- **Cruising:** the ferry sails smoothly in the open water. The speed at this stage is usually at the maximum cruising speed. The trajectory of the cruising phase is

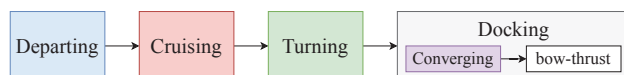


Fig. 4. Decomposing the complete commuting route into scenarios.

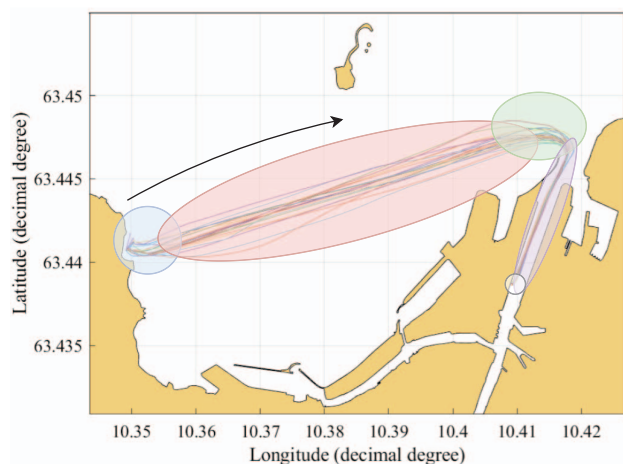


Fig. 5. Decomposition of the commuting route (the color scheme referring to Fig. 4).

almost a straight line without heading variation (except for necessary collision avoidance). Since the pitch angle is proportional to the surge speed, the pitch increases significantly during this stage.

- **Turning:** the ferry changes its course during the sailing. Before making a turn, the ferry will decelerate sharply to a moderate speed, and then the azimuth angle will be steered meticulously to turn the ferry. After the ferry heads the new desired direction, the speed will regain within a certain extent if the channel condition allows.
- **Converging:** the ferry travels in the channel water and gets closer to the coast wall but keeps a safe distance from it. The phase is similar to the cruising stage, but the speed is much lower and the heading may vary slightly as required.
- **Bow thrust:** the ferry pushes itself towards the quay when it arrives at the dock site in a way that is in parallel with the dock wall. The speed at this phase is close to zero. The bow thruster will be turned on, and the azimuth thrusters will adjust their angle to help the ferry to be translational thrust into the quay.

The decomposed route is illustrated on the map as Fig. 5. Only the non-overlapping parts are considered as typical to the decomposed stages or phases, while the overlapping parts will be introduced in the part C.

C. Empirical criteria based on human expertise

Based on the collected data and under the supervision of human expertise, empirical criteria are given as listed in Table II. Basically, since there are several items describing one scenario simultaneously, by which the accuracy has been guaranteed to determine the ferry's status at the moment, the value range of the data is constrained softly to avoid misjudging caused by the common fluctuation of the ship status during a sailing (even in a steady state). For example, the cruising scenario is described by so many feature items

TABLE II
EMPIRICAL CRITERIA FOR THE COMMUTING ROUTE DECOMPOSITION

	Departing	Cruising	Turning	Converging	Bow-thr.
Ship behaviors					
heading (ψ , °)	$\frac{\Delta\psi}{\Delta t} < -0.3$	$ \frac{\Delta\psi}{\Delta t} < 0.1$	$\frac{\Delta\psi}{\Delta t} > 0.5$	$ \frac{\Delta\psi}{\Delta t} < 0.1$	–
grounding speed (v , knot)	≤ 6	≥ 10	$\frac{\Delta v}{\Delta t} < -0.02$	$[4, 6]$	≤ 2
pitch (°)	–	$abs^* > 0.5$	–	$abs > 0$	–
Machinery actuators					
bow thruster (%)	$abs > 0.1$	–	–	–	$abs > 10$
port-rpm (%)	$abs < 60$	$abs > 75$	$abs \in [40, 60]$	$abs \in [40, 60]$	$abs \in [0, 30]$
stbd-rpm (%)	$abs < 60$	$abs > 75$	$abs \in [40, 60]$	$abs \in [40, 60]$	$abs \in [0, 30]$
port-azi (°)	$abs > 0.5$	$abs < 1$	$abs > 0.5$	$abs < 2$	> 50
stbd-azi (°)	$abs > 0.5$	$abs < 1$	$abs > 0.5$	$abs < 2$	$abs < 1$

* abs is the abbreviation of *absolute value*.

(all eight items) that the judgement has been guaranteed to be correct to a certain extent. Hence, some items are constrained softly, such as the grounding speed is relaxed to minimum 10 knots instead of restrict cruising speed. In a word, the number of constraints and the hardness should be balanced well so that empirical criteria are able to decompose the commuter route correctly.

It should be noticed that, suggested by the human expertise, collected data do not reflect distinguishable features between different scenarios for the roll motion, so that data of roll motion are considered as redundant. For the engine status, since the engine is always on, engine data are considered as redundant as well. These two data items are excluded when generating empirical criteria.

D. Transition time window

When the ferry shifts from the current scenario to the next, some necessary operations should be taken to alter the ship motion status in order to meet the sailing requirement. This time window for operations and the ship transferring to a new scenario is defined as a transition time window. The overlapping parts in Fig. 5 are considered as transition time windows. The relationship between the transition time windows and the scenario on the timeline is shown as Fig. 6.

There will be a short period of time in which the status of the ferry is of uncertainty. This means that the ferry status cannot be affirmatively identified as any of pre-defined scenarios. The situation is usually that the ferry status has mutual features of both the pre- and post-scenario. For example, when the ferry shifts from departing to cruising, the main thrusters reach 80% MCR before the heading turns into the desired direction (which is similar to the departing scenario). When the heading is stable, the ferry is yet accelerated to the cruising

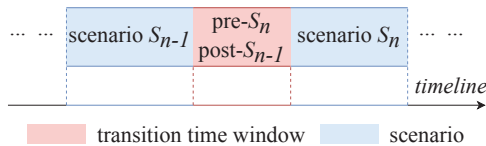


Fig. 6. Transition time windows on the timeline.

speed (which is similar to the cruising scenario). However, there might exist situations where the ferry status is only similar to either the pre-scenario or the following one with noticeable difference; and sometimes the ferry status may be different from neither the pre-scenario nor the following one.

E. Statistical heat map

Statistical method is believed to be able to interpret the decomposed data. The statistical figure is to be calculated and demonstrated by a heat map to help understand how the commuting sailing is regulated by the manual steering with respect to the location. After every commuting sailing is decomposed into scenarios according to empirical criteria, a heat map can be drawn for each scenario accumulatively based on all collected sailings' data. In this case, by transferring collected data points into a heat map, the density of the distribution with respect to the location can be clearly reflected. Thus, sites of likelihood for all scenarios can be qualitatively established. The heat map implies the occurrence possibility of the ferry at each location. The heat map may help to support on-board decisions in the further application.

III. RESULTS

A. Decomposition result by the empirical criteria

The 21 sailings' log data are decomposed according to empirical criteria in Table II. The decomposition result is given in Table III. The decomposition result is denoted in the form (*start time*, *end time*), the unit of time is second. The real period for each scenario (split by the human expertise manually) is listed in columns *Real* as the standard reference. From the form, it is noticed that the decomposition is incomplete in some sailing record. By reviewing the collected data, it is found that the heading was not recorded for sailing No. 5 while the bow thruster feedback was not recorded for sailings No. 20 and 21. During the cruising stage of sailing No.12, the ferry was operated much lower than the rated cruising speed. In sailings No.12 and No.13, the starboard azimuth angles were steered in an abnormal way. Consequently, these 5 groups of sailing data will not be further analyzed.

To understand the decomposition result better, two evaluating terms are defined:

TABLE III
RESULT OF THE SCENARIO DECOMPOSITION BY THE EMPIRICAL CRITERIA*

	Departing		Cruising		Turning		Converging		Bow-thrust	
	E.C.**	Real	E.C.	Real	E.C.	Real	E.C.	Real	E.C.	Real
1	(439,530)	(399,542)	(567,1091)	(566,1098)	(1181,1233)	(1118,1248)	(1253,1531)	(1250,1587)	(1609,1761)	(1603,1794)
2	(1,323)	(1,391)	(404,894)	(404,900)	(901,1044)	(895,1053)	(1055,1351)	(1060,1354)	(1414,1800)	(1382,1659)
3	(307,504)	(322,556)	(552,1033)	(552,1053)	(1074,1135)	(1040,1186)	(1194,1407)	(1196,1547)	(1606,1799)	(1569,1847)
4	(332,352)	(260,466)	(507,931)	(494,949)	(970,1084)	(967,1138)	(1021,1372)	(1177,1434)	(1500,1765)	(1406,1773)
5	—	(178,491)	—	(555,1015)	—	(1038,1178)	—	(1208,1473)	(1528,1763)	(1489,1820)
6	(384,487)	(209,488)	(525,1025)	(523,1031)	(1080,1170)	(1069,1170)	(1210,1514)	(1195,1575)	(1581,1672)	(1580,1803)
7	(125,225)	(108,244)	(268,767)	(259,793)	(860,926)	(816,953)	(943,1294)	(962,1342)	(1343,1751)	(1324,1801)
8	(316,429)	(276,457)	(464,935)	(453,935)	(947,1101)	(941,1106)	(1114,1511)	(1110,1550)	(1577,1797)	(1570,1843)
9	(240,349)	(204,399)	(433,898)	(425,892)	(947,1031)	(930,1046)	(1050,1429)	(1059,1556)	(1567,1620)	(1560,1717)
10	(123,205)	(94,255)	(295,770)	(270,770)	(797,885)	(793,1011)	(1026,1397)	(1034,1401)	(1439,1641)	(1415,1648)
11	(108,221)	(91,242)	(298,809)	(265,814)	(850,874)	(825,911)	(924,995)	(923,1336)	(1394,1677)	(1372,1683)
12	(17,397)	(209,516)	—	(543,1057)	(1063,1079)	(1071,1216)	(1223,1476)	(1248,1478)	—	(1496,1850)
13	(29,91)	(18,161)	(215,690)	(179,693)	(704,861)	(679,802)	(811,1097)	(810,1156)	—	(1163,1614)
14	(326,433)	(237,457)	(467,944)	(463,955)	(981,1141)	(973,1132)	(1175,1396)	(1138,1437)	(1453,1609)	(1440,1696)
15	(291,372)	(200,406)	(416,884)	(415,901)	(932,1031)	(925,1034)	(1048,1392)	(1046,1436)	(1446,1800)	(1449,1650)
16	(244,311)	(126,304)	(357,855)	(349,869)	(863,1018)	(856,1020)	(1026,1350)	(1041,1398)	(1409,1718)	(1407,1720)
17	(486,544)	(329,584)	(605,1072)	(602,1085)	(1108,1232)	(1102,1242)	(1242,1531)	(1287,1530)	(1620,1744)	(1582,1804)
18	(413,500)	(370,502)	(546,1028)	(545,1043)	(1123,1185)	(1110,1188)	(1202,1530)	(1205,1528)	(1588,1719)	(1567,1762)
19	(496,564)	(402,615)	(685,1160)	(683,1164)	(1187,1263)	(1174,1285)	(1292,1541)	(1293,1570)	(1641,1759)	(1635,1788)
20	—	—	(606,1110)	(605,1113)	(1137,1263)	(1124,1268)	(1275,1581)	(1268,1648)	—	—
21	—	—	(254,759)	(253,766)	(782,860)	(781,870)	(874,1457)	(860,1134)	—	—

* The unit of values in the table is second.

** E.C. is the abbreviation of empirical criteria in Table II.

TABLE IV
OVERFLOW RATE OF THE DECOMPOSITION*

	Departing	Cruising	Turning	Converging	Bow-thr.	Overall
1	0	0	0	0	0	0
2	0	0	0	1.7	50.9	9.04
3	6.41	0	0	0.57	0	1.13
4	0	0	0	60.7	0	10.71
6	0	0	0	0	0	0
7	0	0	0	5	0	1.14
8	0	0	0	0	0	0
9	0	1.28	0	1.81	0	1.05
10	0	0	0	2.18	0	0.54
11	0	0	0	0	0	0
14	0	0	5.66	0	0	0.63
15	0	0	0	0	76.12	10.99
16	3.93	0	0	4.2	0	1.44
17	0	0	0	18.93	0	3.43
18	0	0	0	1.55	0	0.41
19	0	0	0	0.4	0	0.09
Overall	0.67	0.08	0.41	4.75	7.12	

* The value is written with percentage (%)

TABLE V
COVERAGE RATE OF THE DECOMPOSITION*

	Departing	Cruising	Turning	Converging	Bow-thr.	Overall
1	63.64	98.5	40	82.49	79.58	82.30
2	82.56	98.79	90.51	98.98	88.45	92.32
3	77.78	96.01	41.78	60.11	69.42	74.70
4	9.71	93.19	66.67	75.88	72.21	69.92
6	36.92	98.43	89.11	80.00	40.81	72.97
7	73.53	93.45	48.18	87.37	85.53	84.44
8	62.43	97.72	93.33	90.23	80.59	87.93
9	55.90	98.29	72.41	74.45	33.76	75.07
10	50.93	95.00	40.37	98.91	86.70	81.81
11	74.83	93.08	27.91	17.19	91.00	66.36
14	48.64	96.95	94.97	73.91	60.94	77.98
15	39.32	96.30	90.83	88.21	100.00	85.70
16	33.71	95.77	94.51	86.55	98.72	86.88
17	22.75	96.69	89.21	100.00	55.86	75.71
18	65.91	96.79	79.49	100.00	67.18	88.50
19	31.92	98.75	68.47	89.53	77.12	79.76
Overall	51.71	96.46	70.52	80.29	76.35	

* The value is written with percentage (%)

- **Overflow rate:** when the judgement result by the empirical criteria is out of the real scenario scale, the judgement is regarded as an overflow value. Then the overflow rate is calculated by dividing the total number of overflow value by the scenario's real time span. Smaller overflow rate indicates better decomposition performance. The result is given in Table IV.
- **Coverage rate:** when the judgement result by the empirical criteria is in the real scenario scale, the judgement is said to be a candidate of coverage. Then the coverage rate is calculated by dividing the total number of coverage candidates by the scenario's real time span. Larger cover-

age rate indicates better decomposition performance. The result is given in Table V.

Tab. IV implies that the decomposition by the empirical criteria is, to some extent, conservative in the scenarios of departing, cruising and turning. It is conservative in the scenario of bow-thrusting as well in most cases, with only sailings No.2 and No.15 having a large overflow rate, which contributes to the overall rate. The overflow happens more frequently in the converging phase than other scenarios, but the rate is acceptable in most cases while is conspicuous large in sailing No.17 and exaggerated large in sailing No.4.

According to Table V, it reveals that the decomposition

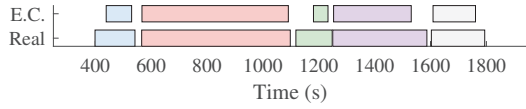


Fig. 7. Decomposition of sailing No.1 (color scheme referring to Fig. 4). E.C. is abbreviated for empirical criteria.

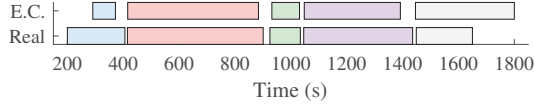


Fig. 8. Decomposition of sailing No.15 (color scheme referring to Fig. 4). E.C. is abbreviated for empirical criteria.

by the empirical criteria has a good coverage performance in most scenarios. The coverage rate of the cruising scenario is 96.46% which suggests that the decomposition reflects the real situation almost entirely. The coverage rate is relatively lower in departing scenario. One reason behind it might be the great complexity of the scenario, for example, sometimes it requires the ferry to use the bow thruster to push it out of the port while sometimes not. The complexity somehow increases the difficulty to correctly extract the whole scenario from the timeline by the empirical criteria.

Take sailings No.1 and No.15 for example. The decomposition results are depicted as Fig. 7 and Fig. 8 respectively. The blank intervals between each two scenarios are transition time windows defined in Sec. II. The two examples prove that the decomposition result is conservative in most scenarios. However, the detail of the overflow in Fig. 8 happening in the bow thrusting phase is that the empirical criteria misjudges the phase for a long time when the phase ends. This might be that due to the effect of the current and/or wind, the bow thruster and the azimuth angles of the main thrusters keep functioning to hold its position even after the ferry has reached the berthing point.

Based on effective log data from 16 sailings, the statistical heat maps are drawn according to the decomposition by the empirical criteria. The heat maps depicting the likelihood sites of each scenario or phase are shown in Fig. 9-13 (departing,

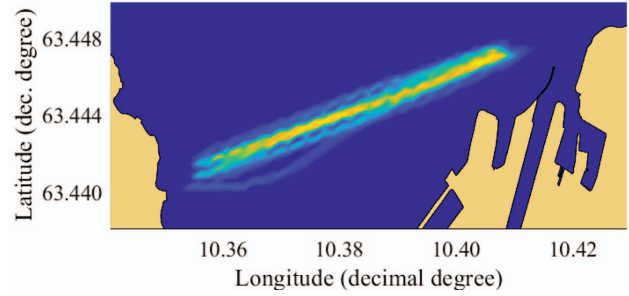


Fig. 10. Heat map presenting the likelihood site of the cruising scenario.

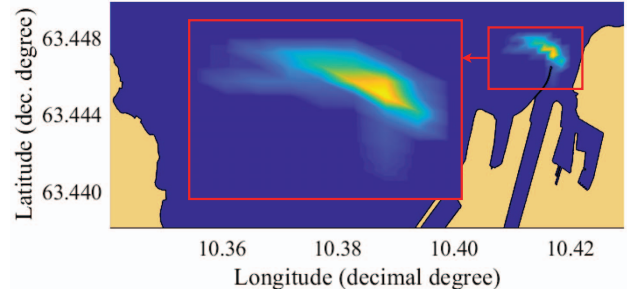


Fig. 11. Heat map presenting the likelihood site of the turning scenario.

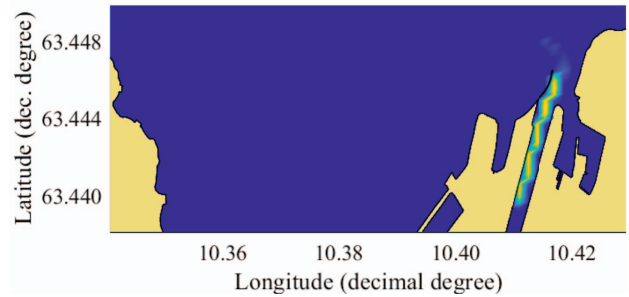


Fig. 12. Heat map presenting the likelihood site of the converging phase.

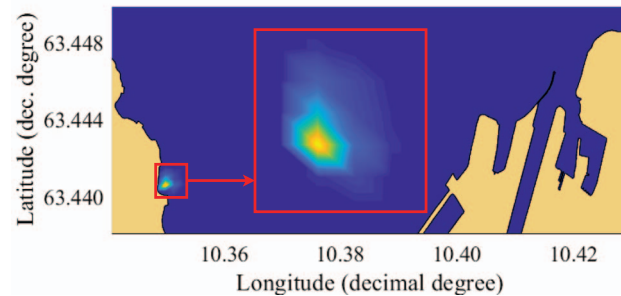


Fig. 9. Heat map presenting the likelihood site of the departing scenario.

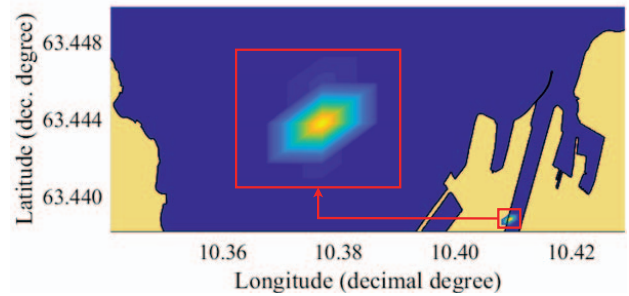


Fig. 13. Heat map presenting the likelihood site of the bow thrusting phase.

cruising, turning scenarios and converging, bow thrusting phases respectively).

In general, there is a kernel in the likelihood site of each scenario or phase, which implies that the ferry passes the kernel area with the largest possibility according to the historical log data. The likelihood site of each scenario or phase is constrained in a certain area and does not overlap with the likelihood sites of other scenarios or phases. This suggests that the decomposition by the empirical criteria performs well to distinguish different sailing scenarios.

From the heat maps, more details are explored and represented. In Fig. 10, the kernel at the tail (upper right of the track) is more condensed than at the head (lower left of the track). The reason is that the ferry begins to decelerate, which then render itself leaving more tracing points in the late phase of the cruising scenario.

IV. DISCUSSION

From the result, a qualitative relationship between the ship status (determined by empirical criteria) and the location is clearly reflected by heat maps. Heat maps illustrate likelihood sites of different scenarios, which can be considered to facilitate the on-board decision support system. Since there are necessary maneuvering operations in each scenario, if they are not executed when the ferry enters the corresponding likelihood site, the decision support system will alarm. In another respect, since heat maps are obtained statistically, they can assist to determine the optimal path for the commuting route. However, the quantity of data being analyzed in this Trondheim commuter route is relatively small. With more data volume, the likelihood site may attain a higher resolution, and be quantitatively determined.

V. CONCLUSION

This paper presents a method to interpret the log data from a commuter ferry. The proposed method aims to construct the mechanism of how human expertise steers a ferry, and then model the mechanism as criteria to judge the status of the ship during a sailing. The model criteria can thus be used to support on-board decisions. As the commuting route is considered as a promising application for ship intelligence, the method is implemented on a customized commuting route in Trondheim. In order to establish the empirical criteria model, human expertise's advice is taken into account to define different sailing scenarios in the commuting route. At last, the decomposition result is demonstrated by statistical method to help better understand the mechanism of operating a commuting ferry. The qualitative relationship between the on-board actuators' action and ship response is thus established to cooperatively judge the status of the ferry.

ACKNOWLEDGMENT

Thanks to the operation team of R/V Gunnerus vessel for advisory cooperation and conducting the customized commuting route. Thanks to Robert Skulstad at Department of Ocean Operations and Civil Engineering at NTNU for his contribution on the data collecting and delightful discussion.

REFERENCES

- [1] T. Porathe, Å. S. Hoem, Ø. J. Rødseth, K. E. Fjørtoft, and S. O. Johnsen, "At least as safe as manned shipping? autonomous shipping, safety and "human error",", *Safety and Reliability-Safe Societies in a Changing World. Proceedings of ESREL 2018, June 17-21, 2018, Trondheim, Norway*, 2018.
- [2] A. M. Rothblum, "Human error and marine safety," in *National Safety Council Congress and Expo, Orlando, FL*, no. s 7, 2000.
- [3] E. Jokioinen, J. Poikonen, R. Jalonen, and J. Saarni, "Remote and autonomous ships-the next steps," *AAWA Position Paper, Rolls Royce plc, London*, 2016.
- [4] M. Hinostroza and C. G. Soares, "Collision avoidance, guidance and control system for autonomous surface vehicles in complex navigation conditions," in *Progress in Maritime Technology and Engineering: Proceedings of the 4th International Conference on Maritime Technology and Engineering (MARTECH 2018), May 7-9, 2018, Lisbon, Portugal*. CRC Press, 2018, p. 121.
- [5] Ø. J. Rødseth and H. C. Burmeister, "Developments toward the unmanned ship," in *Proceedings of International Symposium Information on Ships-ISIS*, vol. 201, 2012, pp. 30–31.
- [6] L. A. Nguyen, M. D. Le, S. H. Nguyen, T. H. H. Nghiem *et al.*, "A new and effective fuzzy pid autopilot for ships," in *SICE 2003 Annual Conference (IEEE Cat. No. 03TH8734)*, vol. 3. IEEE, 2003, pp. 2647–2650.
- [7] L. Perera, J. Carvalho, and C. G. Soares, "Fuzzy logic based decision making system for collision avoidance of ocean navigation under critical collision conditions," *Journal of marine science and technology*, vol. 16, no. 1, pp. 84–99, 2011.
- [8] M. R. Benjamin, J. J. Leonard, J. A. Curcio, and P. M. Newman, "A method for protocol-based collision avoidance between autonomous marine surface craft," *Journal of Field Robotics*, vol. 23, no. 5, pp. 333–346, 2006.
- [9] M. Tannum and J. Ulvensøen, "Urban mobility at sea and on waterways in norway," in *Journal of Physics: Conference Series*, vol. 1357, no. 1. IOP Publishing, 2019, p. 012018.
- [10] M. J. Lewandowski, M. Fitzpatrick, and N. F. Kamradt, "Maritime mass rescue interventions: Availability and associated technology," COAST GUARD NEW LONDON CT RESEARCH AND DEVELOPMENT CENTER, Tech. Rep., 2010.
- [11] W. C. Tan, C.-Y. Weng, Y. Zhou, K. H. Chua, and I.-M. Chen, "Historical data is useful for navigation planning: Data driven route generation for autonomous ship," in *2018 IEEE International Conference on Robotics and Automation (ICRA)*. IEEE, 2018, pp. 7478–7483.
- [12] S. Mao, E. Tu, G. Zhang, L. Rachmawati, E. Rajabally, and G.-B. Huang, "An automatic identification system (ais) database for maritime trajectory prediction and data mining," in *Proceedings of ELM-2016*. Springer, 2018, pp. 241–257.
- [13] A. L. Ellefsen, X. Cheng, F. T. Holmeset, V. Æsøy, H. Zhang, and S. Ushakov, "Automatic fault detection for marine diesel engine degradation in autonomous ferry crossing operation," in *2019 IEEE International Conference on Mechatronics and Automation (ICMA)*. IEEE, 2019, pp. 2195–2200.
- [14] A. L. Ellefsen, V. Æsøy, S. Ushakov, and H. Zhang, "A comprehensive survey of prognostics and health management based on deep learning for autonomous ships," *IEEE Transactions on Reliability*, vol. 68, no. 2, pp. 720–740, 2019.
- [15] G. Li, R. Mao, H. P. Hildre, and H. Zhang, "Visual attention assessment for expert-in-the-loop training in a maritime operation simulator," *IEEE Transactions on Industrial Informatics*, 2019.
- [16] L. P. Perera, B. Mo, L. A. Kristjánsson, P. Jonvik, and J. Svardal, "Evaluations on ship performance under varying operational conditions," in *Proceedings of the 34th International Conference on Ocean, Offshore and Arctic Engineering (OMAE 2015), Newfoundland, Canada, (OMAE2015-41793)*, 2015.
- [17] (2006) Specifications of ntnu's research vessel r/v gunnerus. [Online]. Available: <https://www.ntnu.edu/c/documentlibrary/getfile?uuid=4b1280ed-378a-4715-bf34-5c33c340f01egroupId=919518>